THE JOURNAL OF BIOLOGICAL CHEMISTRY
Vol. 278, No. 45, Issue of November 7, pp. 44708–44718, 2003

Printed in U.S.A.

Ether Phospholipids and Glycosylinositolphospholipids Are Not Required for Amastigote Virulence or for Inhibition of Macrophage Activation by *Leishmania major**

Received for publication, July 24, 2003, and in revised form, August 25, 2003
Published, JBC Papers in Press, August 27, 2003, DOI 10.1074/jbc.M308063200

Rachel Zufferey‡§, Simon Allen¶‖, Tamara Barron, Deborah R. Sullivan**, Paul W. Denny‡‡, Igor C. Almeida§§, Deborah F. Smith‡‡, Salvatore J. Turco**, Michael A. J. Ferguson¶, and Stephen M. Beverley‡¶¶**

*From the ‡Department of Molecular Microbiology, Washington University School of Medicine, St. Louis, Missouri 63110, the ¶Wellcome Trust Biocentre, University of Dundee, Dundee DD1 4HN, Scotland, United Kingdom, the **Department of Biochemistry, University of Kentucky Medical Center, Lexington, Kentucky 45306, the ‡‡Department of Biological Sciences, Wellcome Trust Laboratories for Molecular Parasitology, Imperial College, London SW7 1AZ, United Kingdom, and the §§Department of Parasitology, Universidade de Sao Paulo, Sao Paulo 05508-900, Brazil*

Ether phospholipids are major components of the membranes of humans and *Leishmania*. In protozoan parasites they occur separately or as part of the glycosylphosphatidylinositol (GPI) anchor of molecules implicated in virulence, such as lipophosphoglycan (LPG), smaller glycosylinositolphospholipids (GIPLs), and GPI-anchored proteins. We generated null mutants of the *Leishmania major* alkyldihydroxyacetonephosphate synthase (ADS), the first committed step of ether lipid synthesis. Enzymatic analysis and comprehensive mass spectrometric analysis showed that *ads1*$^-$ knock-outs lacked all ether phospholipids, including plasmalogens, LPG, and GIPLs. *Leishmania ads1*$^-$ thus represents the first ether lipid-synthesizing eukaryote for which a completely null mutant could be obtained. Remarkably *ads1*$^-$ grew well and maintained lipid rafts (detergent-resistant membranes). In virulence tests it closely resembled LPG-deficient *L. major*, including sensitivity to complement and an inability to survive the initial phase of macrophage infection. Likewise it retained the ability to inhibit host cell signaling and to form infectious amastigotes from the few parasites surviving the establishment defect. These findings counter current proposals that GIPLs are required for amastigote survival in the mammalian host or that parasite lyso-alkyl or alkylacyl-GPI anchors are solely responsible for inhibition of macrophage activation.

The surface of the *Leishmania* parasite is a major point of interaction with the host throughout the infectious cycle, which includes an extracellular promastigote form residing in the midgut of sand flies and an intracellular amastigote form adapted for survival within the phagolysosomes of vertebrate macrophages. Glycosylphosphatidylinositol (GPI)[1]-anchored molecules dominate the parasite surface, and many of these have been implicated in the ability of the parasite to survive in such hostile environments (1). Abundant surface molecules include lipophosphoglycan (LPG, containing 15–30 copies of a phosphoglycan (PG) repeating unit), GPI-anchored proteins such as membrane proteophosphoglycans, gp63 and gp46, and a heterogeneous group of small glycosylinositolphospholipids (GIPLS; for reviews, see Refs. 2 and 3).

LPG, GIPLs, and related molecules have been shown to inhibit activation and signaling when applied exogenously to macrophages (4–7). The expression of LPG and GPI-anchored proteins decreases greatly in intracellular amastigotes, while GIPLs remain at high levels (2, 8). These and other data have led to proposals that GIPLs are key molecules for survival of amastigotes within the macrophage phagolysosome (9–11).

A shared structural motif of GPI-anchored glycoconjugates as well as other abundant phospholipids in *Leishmania* is the presence of ether lipids. The lipid moieties of GIPLs and GPI-anchored proteins are *sn*-1-alkyl-2-acyl-PIs (for reviews, see Refs. 1–3) while that of LPG is *sn*-1-alkyl-2-lyso-PI where the alkyl group is C_{24-26} (12, 13). The GPI anchors of GIPLs and LPG with its very long chain alkyl group have been implicated in down-regulation of host cell responses, for example in the inhibition of protein kinase C and nitric oxide (NO) production (5, 14–16). At least 10% of the total membrane lipids in *Leishmania* consist of ether lipids within GPI anchors or in phospholipids including phosphatidylethanolamine (PE), phosphatidylcholine (PC), and phosphatidylserine (17–19). Ether lipid analogs have strong inhibitory activity against parasites exemplified by the recent introduction of miltefosine into clinical usage against *Leishmania donovani* (for a review, see Ref.

* This work was supported by a Human Frontier Science Program Organization grant (to R. Z.), Wellcome Trust Program Grants 054491 and 061343 (to M. A. J. F. and D. F. S., respectively), a Biotechnology and Biological Sciences Research Council Ph.D. studentship (to S. A.), Conselho Nacional de Pesquisas (Brazil) Research Fellowship 98/10495-5 (to I. C. A.), and National Institutes of Health grants (to S. J. T. and S. M. B.). The costs of publication of this article were defrayed in part by the payment of page charges. This article must therefore be hereby marked "*advertisement*" in accordance with 18 U.S.C. Section 1734 solely to indicate this fact.

The nucleotide sequence(s) reported in this paper has been submitted to the GenBank™/EBI Data Bank with accession number(s) AY328521.

§ Present address: Dept. of Pathology and Center for Microbial Pathogenesis, University of Connecticut Health Center, Farmington, CT 06032.

‖ Present address: Buck Inst., 8001 Redwood Blvd., Novato, CA 94945.

¶¶ To whom correspondence should be addressed: Dept. of Molecular Microbiology, Campus Box 8230, Washington University Medical School, 660 S. Euclid Ave., St. Louis, MO 63110. Tel.: 314-747-2630; Fax: 314-747-2634; E-mail: beverley@borcim.wustl.edu.

[1] The abbreviations used are: GPI, glycosylphosphatidylinositol; LPG, lipophosphoglycan; ADS, alkyldihydroxyacetonephosphate synthase; DRM, detergent-resistant membrane; GIPL, glycosylinositolphospholipid; PG, phosphoglycan; PI, phosphatidylinositol; sAP, secretory acid phosphatase; DHAP, dihydroxyacetonephosphate; PE, phosphatidylethanolamine; PC, phosphatidylcholine; WT, wild type; ES-MS, electrospray mass spectrometry; GFP, green fluorescent protein; CID, collision-induced dissociation; ES-MS-CID-MS, electrospray tandem mass spectrometry with collision-induced dissociation.

20). In mammals ether phospholipids constitute nearly 20% of total phospholipids, occurring most commonly as 1-*O*-alkenyl-2-alkyl-*sn*-glycero-3-phosphocholine or phosphoethanolamine plasmalogens (for a review, see Ref. 21). Plasmalogens have been implicated in signal transduction, membrane fusion and trafficking, oxidant resistance, and prostaglandin synthesis (for a review, see Ref. 21).

To focus on the question of the role of the lipid moiety of GPI anchors in the infective cycle, we took a genetic approach targeting alkyldihydroxyacetonephosphate synthase (ADS, EC 2.5.1.26), the first committed step in ether lipid synthesis. In *Leishmania* as in other organisms, this pathway begins with the acylation of dihydroxyacetonephosphate (DHAP) followed by replacement of the acyl group with an alkyl group and then reduction to give the ether lipid precursors 1-alkylglycerol-3-phosphate (22, 23). In mammals this pathway occurs in peroxisomes, while in trypanosomatids it occurs in glycosomes, a microbody variant of peroxisomes (for reviews, see Refs. 22 and 24). ADS activity has been characterized, and its gene has been identified in a number of species including *Trypanosoma brucei* (22, 23, 25, 26). We used this information to identify the *Leishmania* gene *ADS1* and to create null mutants to assess the role of ether lipids in parasite metabolism and virulence.

EXPERIMENTAL PROCEDURES

Parasite Culture—Leishmania major Friedlin strain V1 (MHOM/IL/80/Friedlin) promastigote forms were cultivated in M199 medium at 26 °C and transfected by electroporation (27). As needed, G418, hygromycin, nourseothricin, or puromycin were added at 10, 50, 100, and 50 μg/ml, respectively. Metacyclic promastigotes were prepared by Ficoll gradient centrifugation (28).

Molecular Biology—All enzyme restriction reactions, PCR, and DNA and RNA extractions and hybridizations (Southern blot, Northern blot, and colony hybridization) were performed by standard methods (29). DNA hybridization probes were made using a random priming kit (Roche Applied Science). The gene *D/SHERP* probe was obtained by PCR from genomic DNA with primers Y09088 137–156 (5′-GATCCGCGCAGACCAAGATG) and Y09087 320–300 (5′-CAGAGAACGGCGAAGGGACTG). For reverse transcriptase PCR, cDNA was prepared from RNA isolated from logarithmic phase promastigotes using random primers for the reverse transcription reaction (Invitrogen) and used as template for PCR with an oligonucleotide specific for the miniexon (SMB936, 5′-ACCGCTATATAAAGTATCAGTTCTGTACTTTA) and one specific for *ADS1* (either SMB1012, 5′-ACTAGTGCTGTCCTGTGTTTTATCG, located in the 5′ untranslated region, or SMB1017, 5′-ATCTGCATCTGGACATCC, located within the *ADS1* coding region). These products were directly sequenced by the chain termination method.

Cloning of ADS1 of L. major and Plasmid Construction—A 1.58-kb fragment was obtained following PCR with *L. major* genomic DNA template and the *ADS1* degenerate primers SMB929 (5′-AAGTGGAAYGGNTGGGG) and SMB931 (5′-CCSATNCCGTGGTGGTGNGT). This was inserted into pCR2.1 (Invitrogen) to give pCRII.DHAP-PCR (strain B3772) and sequenced. This PCR product was used to screen a *L. major* Friedlin strain V1 cLHYG cosmid library (30) by colony hybridization. Positive clones were further analyzed by restriction enzyme digestion followed by Southern blot analysis probed with the 1.58-kb PCR product. A 3.6-kb SphI fragment containing *ADS1* was cloned into pUC19 yielding pUC.DHAP.Sp1 (B3793) and sequenced on both strands.

Plasmids for inactivation of *ADS1* were generated as follows from pUC.DHAP.Sp1 (B3793) that carries a 3.6-kb SphI fragment containing the entire *ADS1* gene and flanking regions. The 1.7-kb SphI-Eco47III fragment (blunt-ended) of the *ADS1* open reading frame was replaced with the *HYG* or *SAT* cassettes as SpeI-AflII fragments (blunt-ended, 2.2 and 1.8 kb, respectively) excised from pX63HYG (31) or pXGSAT (B2352). pXGSAT was constructed by replacing the *NEO* marker with a PCR-amplified (SMB248, 5′-CGACTAGTTAGCCGTCATCCTGTGC; SMB249, 5′-GTGACTAGTATGAAGATTTCGGTGATCC) SAT cassette from pLEXSAT (32) cloned in the SpeI site of pXG1a (33), respectively. The plasmids carrying the resistance marker in the same transcription orientation as the *ADS1* gene were kept and named pUC.DHAP:HYGΔSS (B3796) and pUC.DHAP:SAT-BΔSS (B3828), respectively.

pXG-ADS1 and pXG-GFP-ADS1 (B3909 and B4187, respectively) were made as follows. BamHI sites at the 5′ and 3′ ends of the *ADS1* gene were introduced successively by PCR and cloning to yield pUC.B-DHAP-B (B3840). The *ADS1* BamHI fragment was ligated in the sense orientation into the BamHI site of pXG (33) or pXG-GFP^{2+}/ (B2952). pX63PAC-LdSAcP-1 (B4191) was obtained by inserting a sense blunt-

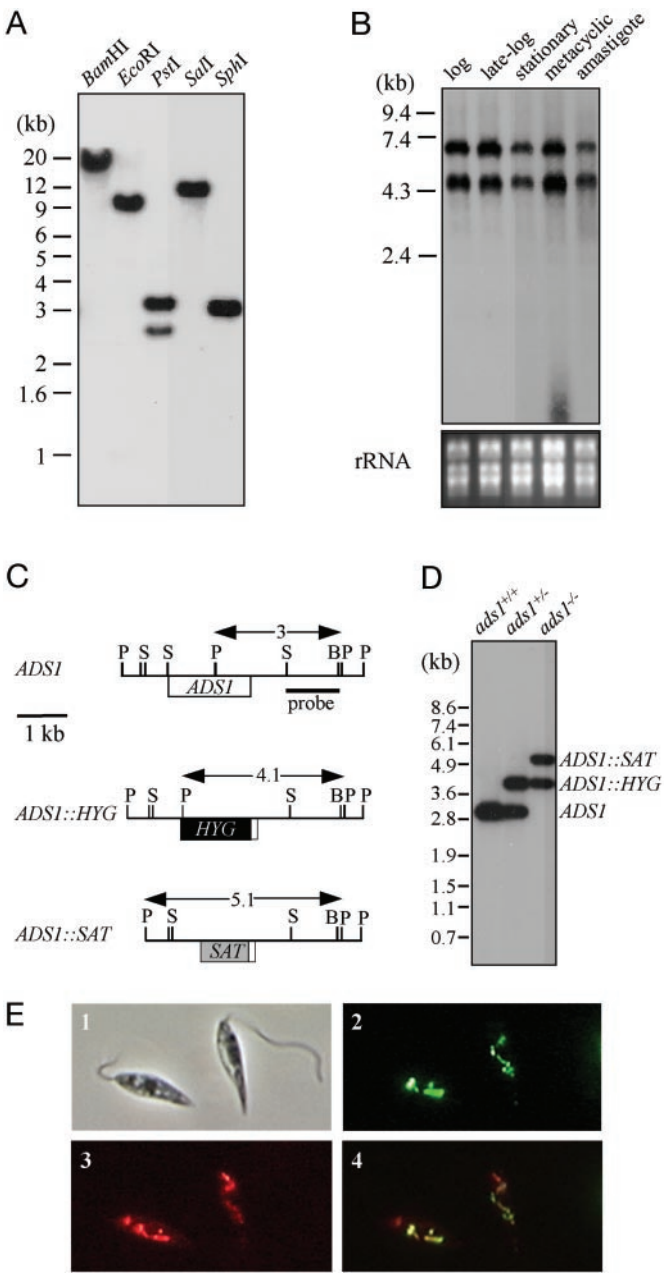

FIG. 1. **Characterization of *ADS1* and *ads1*$^-$ knock-outs.** The migration of size markers (kb) is shown. *A*, Southern blot analysis with WT *L. major* DNA (3 μg) digested with single (PstI) or null enzymes (BamHI, EcoRI, SalI, and SphI). The probe was an *ADS1* PCR fragment obtained with primers SMB929 (5′-AAGTGGAAYGGNTGGGG) and SMB931 (5′-CCSATNCCGTGGTGGTGNGT). *B*, Northern blot analysis with total *L. major* RNAs (5 μg) from log, late log, and stationary promastigotes, metacyclic promastigotes, and lesion amastigotes. The probe is described in *A*. *C*, restriction maps of *ADS1* locus in WT and *ads1*$^-$ replacement lines. The sizes (in kb) expected following PstI digestion and hybridization with a flanking 1-kb SphI-BamHI probe (*black bar*) are shown by *arrows* above each map. *P*, *B*, and *S* indicate PstI, BamHI, and SphI sites, respectively. *D*, Southern blot of PstI-digested DNA from WT (*ads1*$^{+/+}$), heterozygote (*ads1*$^{+/-}$), and homozygote (*ads1*$^{-/-}$) mutants. The probe was shown in *C*. *E*, ADS1 is targeted to the glycosomes. The cells shown are permeabilized WT *L. major* transfected with pXG-GFP-ADS1. *1*, phase microscopy image; *2*, GFP fluorescence (WT controls showed no signal); *3*, indirect immunofluorescence with anti-hypoxanthine guanine phosphoribosyltransferase antiserum; *4*, superposition of 2 and 3.

TABLE I
Growth, differentiation, and serum sensitivity of WT and ads1⁻ mutant L. major

All four assays were done twice in triplicate. S.D. is indicated. ND, not determined.

	WT	*ads1⁻*	*ads1⁻/+ADS1*
Percentage of metacyclic promastigotes (after 4 days in stationary phase)	4.5 ± 0	5.6 ± 0.8	ND
Percentage of human serum (complement) required for 50% lysis (IC_{50})	6.3 ± 1.8	1.0 ± 0.04	6 ± 2.4
Promastigote doubling time *in vitro* (h)	7 ± 0.35	8.1 ± 0.5	ND
Amastigote doubling time in macrophages (days)	1.8 ± 0.2	5.1 ± 0.7	2.0 ± 0.1

ended 3-kb NcoI-PstI fragment from pLdSAcP3.9 (34) into the BamHI site of pX63PAC (B2949).

Western Blot Analysis—Leishmania were first washed once in PBS (136 mM NaCl, 2.7 mM KCl, 8.5 mM KH_2PO_4, 1 mM Na_2HPO_4, pH 7.2) and then lysed in SDS-PAGE loading dye (2% SDS (w/v), 0.7 M β-mercaptoethanol, 10% glycerol, 62 mM Tris-HCl, pH 6.8, 0.05% bromphenol blue). The samples were heated for 15 min at 70 °C and loaded on discontinuous 4%/10% SDS-polyacrylamide gels. Proteins were transferred to nitrocellulose filters by the Towbin method. Preincubation, antibody incubations, and washes were conducted in TBST buffer (10 mM Tris-HCl, pH 8, 150 mM NaCl, 0.05% Tween 20) with 5% skim milk added. Detection was performed with a chemiluminescence kit (ECL, Amersham Biosciences) followed by autoradiography.

Enzyme Assays—ADS activity was measured in an enriched glycosome fraction using slight modifications of the protocol by Heise *et al.* (22). Cells were resuspended in 7 ml containing 0.25 M sucrose, 1 mM EDTA, and 25 mM Tris-HCl, pH 7.8 (STE buffer) and disrupted by nitrogen cavitation (1500–2000 p.s.i. for 30 min at 4 °C). Cellular debris were removed by centrifugation at 1000 × *g* for 10 min, and the supernatant was briefly sonicated. The sample was mixed with 80% Percoll, 20% STE buffer to a final volume of 40% Percoll and centrifuged at 70,000 × *g* in a Beckman NVI90 rotor for 30 min at 4 °C. Glycosome fractions banding at a density of 1.09–1.1 g/ml were taken. Protein concentration was determined according to the bicinchoninic acid assay with a bovine serum albumin standard. Alkyl-DHAP synthase activity was measured in triplicate as described previously with slight modifications (26). Briefly, 0.4 mg of glycosomal proteins were incubated in 100 μl containing 50 mM potassium phosphate, pH 8.0, 100 μM [^{14}C]hexadecanol, 90 μM palmitoyl-DHAP, 1 mM dithiothreitol, 50 μM NaF, 0.1% Triton X-100, 2 μg/ml pepstatin, 2 μg/ml leupeptin, and 10 μg/ml trypsin inhibitor at 37 °C for 40 min and extracted with chloroform:methanol (1:2, v/v) (35). The organic phase was dried under nitrogen, spotted onto silica gel 60 plates, and resolved in solvent chloroform, methanol, acetic acid, 5% sodium bisulfite (100:40:12:4, v/v/v/v); bands were visualized with Lester reagent (36), and the radioactivity in bands with $\sim R_F$ of 3.5 was measured by scintillation counting.

For secretory acid phosphatase assay cell supernatants were loaded on a non-denaturing polyacrylamide gel in the absence of SDS (37); separating and stacking gels were 6 and 3% acrylamide, respectively. Acid phosphatase was visualized as described previously (38).

Microscopy—Indirect immunofluorescence microscopy with anti-hypoxanthine guanine phosphoribosyltransferase antibody was performed as described previously (39). Immunofluorescence and flow cytometry with WIC79.3 antibodies (40) and gp46 were performed according to Ref. 41.

For transmission electron microscopy, parasites were washed in 0.1 M cacodylate buffer, pH 7, and fixed in 2.5% glutaraldehyde (electron microscopy grade, Sigma) in cacodylate buffer containing 5 mM $CaCl_2$, 5% sucrose, and 0.15% ruthenium red (Electron Microscopy Sciences, Ft. Washington, PA) for 1 h at 4 °C. Following three washes in cacodylate buffer, parasites were postfixed in 1% osmium tetroxide (Polysciences Inc., Warrington, PA), 2 mM $CaCl_2$, 0.15% ruthenium red in cacodylate buffer for 1 h at room temperature. The samples were then rinsed extensively in cacodylate buffer, 3% sucrose and deionized water prior to staining with 1% uranyl acetate. Following several rinses in deionized water, samples were dehydrated in a graded series of ethanol and embedded in Spurrs resin (Electron Microscopy Sciences). Sections of 70–80 nm were cut, stained with lead citrate, and viewed on a Zeiss 902 transmission electron microscope.

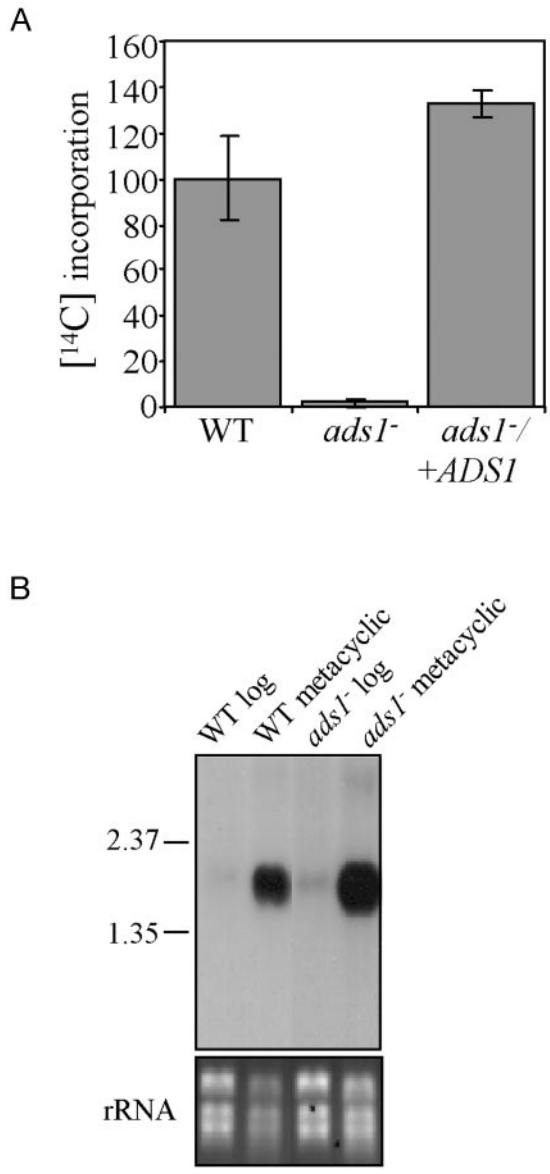

FIG. 2. **Characterization of ADS activity and metacyclogenesis in an *ads1⁻* null mutant.** *A*, enzymatic assay of ADS activity of indicated lines. Assays were performed in triplicate and normalized to WT; the S.D. is shown. *ads1⁻* were identical to background. *B*, Northern blot analysis of total RNAs (5 μg) from procyclic and metacyclic promastigotes of WT and *ads1⁻* cells hybridized with a *SHERP* probe.

Phospholipid, GIPL, and LPG Analysis—Bulk phospholipids and GIPLs were purified and analyzed by electrospray mass spectrometry (ES-MS) in positive and negative ion modes as described previously (10, 42). Phospholipids were dissolved in chloroform:methanol (1:2, v/v) (approximately 2×10^6 cell eq/μl) and introduced into the electrospray source of the mass spectrometer (Quattro triple quadrupole, Micromass) at 5 μl/min with a syringe pump. Parameters were as follows: skimmer/cone offset 5 V; capillary, high voltage lens, and cone voltages, 3 kV, 0.5 kV, and 25 V, respectively for positive ion mass spectra and 3 kV, 0.5 kV, and 45 V for negative ion mass spectra. CID spectra were achieved in a hexapole collision cell containing argon (2.5×10^{-3} torrs). Parent ion spectra were taken using the following accelerating voltages into the collision cell: parents of *m/z* 184 (for PC detection), 27 V (positive ion mode); parents of *m/z* 241 (for PI detection), 45 V (negative ion mode); neutral loss of *m/z* 141 (for detection of PE), 12 V (positive ion mode); and neutral loss of *m/z* 185 (for detection of phosphatidylserine), 27 V (positive ion mode). Daughter ion spectra of $[M - H]^-$ pseudomolecular ions used acceleration voltages of 30–100 V. GIPLs were dissolved in 70% propan-1-ol, 5 mM ammonium acetate at ~20 pmol/μl and introduced into the electrospray source at 5 μl/min using a syringe

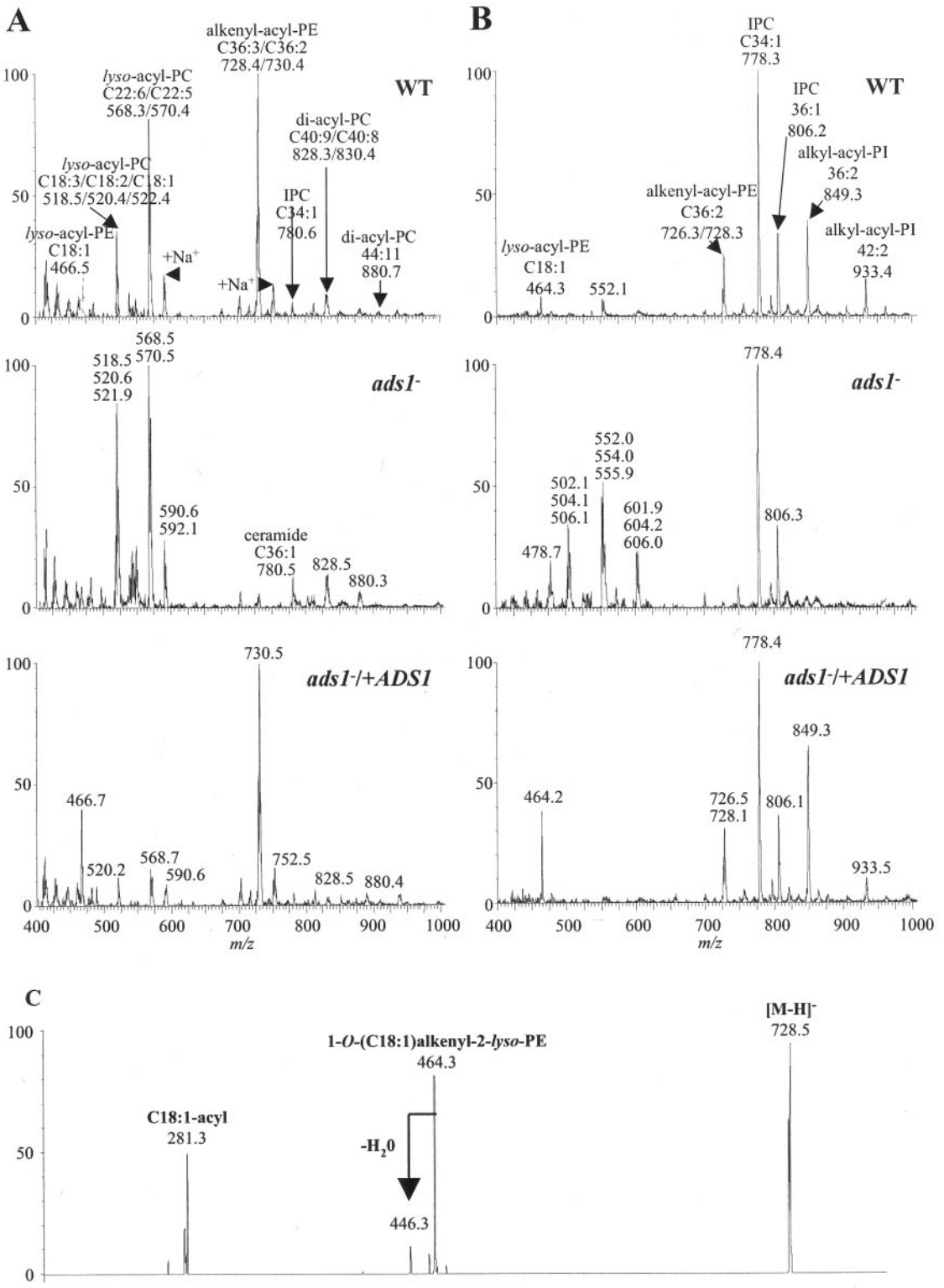

FIG. 3. **The *ads1*⁻ mutant lacks ether phospholipids.** Positive ion (*A*) and negative ion (*B*) ES-MS spectra of total phospholipid fractions purified from wild type (*upper panel*), *ads1*⁻ mutant (*middle panel*), and *ads1*⁻/+*ADS1* parasites (*lower panel*) are shown. Identities of key ions are indicated, and the numbers *X*:*Y* refer to the total number of lipid carbon atoms (*X*) and the degrees of unsaturation (*Y*) in the whole lipid molecule. *C*, negative ion ES-MS-MS daughter ion spectrum of the *m/z* 728 $[M - H]^-$ ion of 1-*O*-alkenyl-2-acyl-PE. IPC, inositol phosphorylceramide.

pump. Samples were analyzed in positive ion mode with a capillary voltage of 3 kV and a cone voltage of 130 V. Daughter ion spectra were collected using an accelerating voltage of 30–100 V. Daughter ion spectra of alkenyl-acyl-PE $[M - H]^-$ pseudomolecular ions were recorded with an LCQ-Duo ion trap electrospray mass spectrometer (Finnigan-Thermoquest, San Jose, CA). Samples were introduced at 5 μl/min. Source voltage and current were 4.52 kV and 0.24 mA, and capillary voltage and temperature were set at 19–36 V and 200 °C. The collision energy was 28% (1.4 eV) under helium pressure. Fragmentation spectra were collected in the *m/z* 175–800 range at a rate of three microscans over a maximum ion injection time of 200 ms.

LPG and the "LPG-like" material in *ads1*⁻ were purified as described previously (13). In some experiments exponentially growing cells were metabolically labeled with [^{3}H]galactose (50 μCi for 8×10^8 cells) for

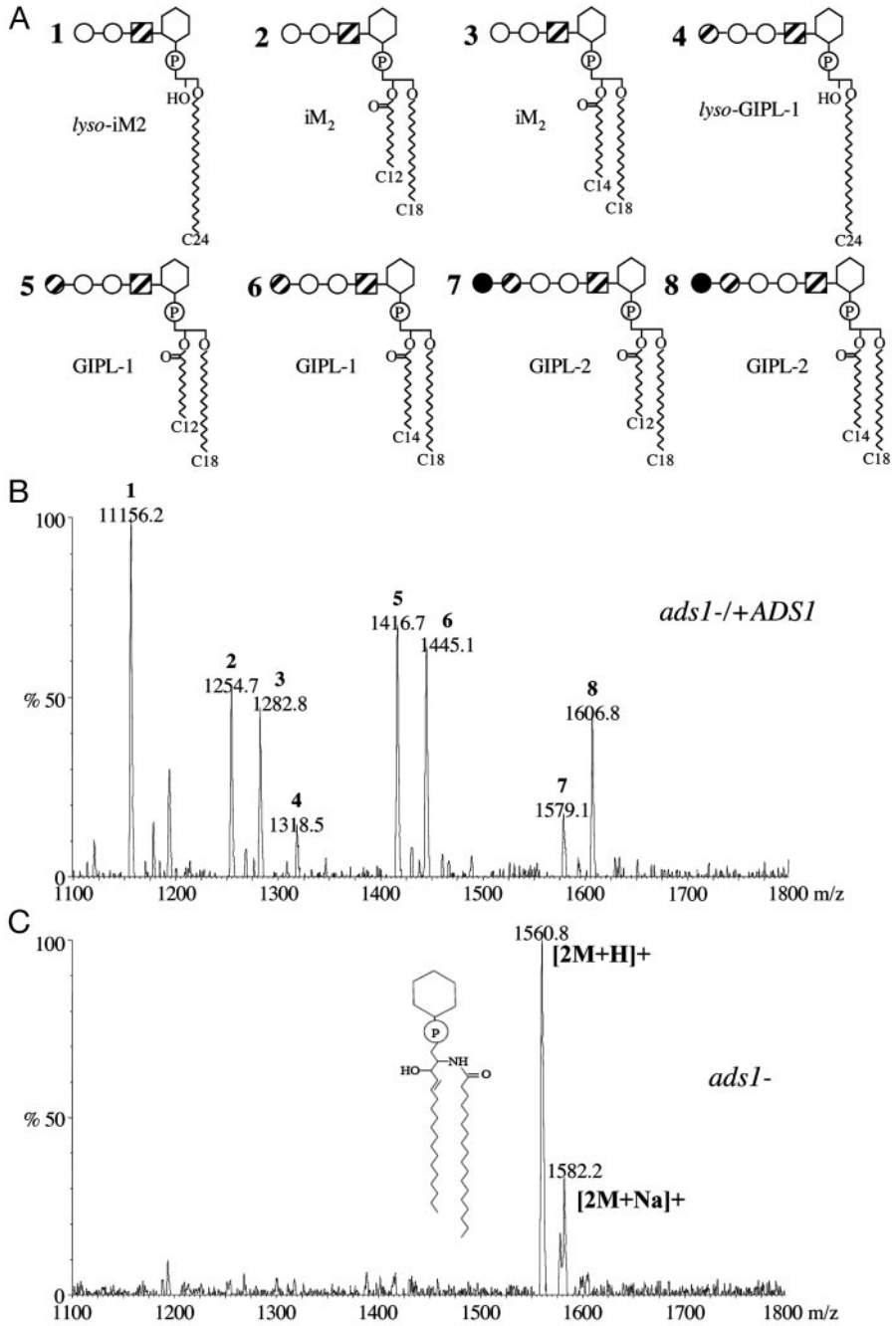

FIG. 4. **The *ads1*$^-$ mutant lacks conventional *L. major* GIPLs.** *A*, the structures of *Leishmania* GIPLs are shown. *B* and *C*, positive ion ES-MS spectrum of GIPL fractions isolated from *ads1*$^-$/+*ADS1* (*B*) and *ads1*$^-$ mutant (*C*) parasites. The identities of the major ions correspond are indicated by schematics in *A* and can be inferred from the structure of GIPL-2 which is: Galα1–6Galα1–3Gal$_f\alpha$1–3Manα1–3Manα1–4GlcNα1–6*myo*-inositol-1-HPO$_3$-3(*sn*-1-alkyl-2-acylglycerol). The structure of the inositol phosphorylceramide species retained in *ads1*$^-$ is shown as an *inset* in *C*. *Solid circles*, Gal$_p$; *hashed circles*, Gal$_f$; *open circles*, Man; *hashed squares*, GlcN; *hexagons*, *myo*-inositol; and *P*, phosphate.

6 h. PG repeat structures were determined from LPG (~50 pmol in 5% propan-1-ol, 5 mM ammonium acetate) by ESI-MS as described previously (43).

Detergent-resistant Membrane (DRM) Preparation and Analysis—Crude membranes were prepared from 10^8 log phase parasites, and DRMs were isolated on a step gradient after extraction with 1% Triton X-100 at 4 °C as described previously (44). Fractions were then taken from the top of the gradient and analyzed by Western blotting.

Mouse and Macrophage Infections—Mice were injected with promastigotes that had been in stationary phase 4 days (1×10^6) or amastigotes (1×10^5) subcutaneously into footpads, and lesion size and parasite numbers were measured (41, 45). *In vitro* infection of peritoneal macrophages was performed as described previously (41, 46). Metacyclic parasites were purified on a Ficoll gradient (28), and crude amastigotes were prepared from lesions (41). Briefly, excised lesions were placed in cold Dulbecco's modified Eagle's medium and dissociated with a Dounce homogenizer, tissue fragments and intact host cells were removed by a low speed centrifugation at $200 \times g$, and amastigotes were pelleted at $1800 \times g$. Amastigotes were washed twice in cold Dulbecco's modified Eagle's medium and then counted with a hemocytometer.

For nitrite quantification, macrophages were induced in the presence of interferon-γ and lipopolysaccharide (100 units and 100 ng/ml, respectively) exactly 4 h after the 2-h wash. Nitrite was quantified 48 h after macrophage induction according to Ref. 47. Lysis by human complement was measured with mid-log phase cultures (5×10^6/ml) incubated with varying amounts of human serum for 30 min at 26 °C (41).

RESULTS

Characterization of L. major ADS1—From known ADS sequences we designed degenerate oligonucleotide primers for amplification of the *L. major* gene and recovered the parasite gene by screening a *L. major* cosmid library. Southern blot analysis showed that the *Leishmania ADS1* gene was single copy (Fig. 1*A*), which was confirmed by targeted gene replacement (described below, Fig. 1*D*). The sequence of the *ADS1* gene predicted a protein of 621 amino acids (GenBank™ accession number AY328521) with strong homology to the ADS proteins of *T. brucei* (59% identity) and other eukaryotes including mammals, *Caenorhabditis elegans*, and *Dictyostelium* (30–37% identity).

ADS1 lacked obvious transmembrane domains but contained at its C terminus the sequence SHI, which resembled typical type 1 peroxisomal targeting signals (PTS1, Ref. 48). We created an N-terminal GFP-ADS1 fusion protein, which was shown to be enzymatically active following transfection into *ads1*$^-$ null mutants (below and data not shown). Fluorescence microscopy showed that GFP-ADS1 fusion protein was correctly targeted to the *Leishmania* glycosome (analogous to peroxisomes of other creatures) and co-localized with the glycosomal marker hypoxanthine guanine phosphoribosyltransferase (Fig. 1*E* and Ref. 39).

In trypanosomatids mRNAs bear a 39-nucleotide 5′-terminal exon added by *trans*-splicing (49). Reverse transcriptase PCR with miniexon and *ADS1*-specific primers mapped the splice acceptor site to nucleotide position −355 relative to the predicted *ADS1* initiation codon. Northern blot analysis showed that *ADS1* mRNA was expressed at similar levels in all developmental stages as two transcripts of 4.6 and 6.6 kb (Fig. 1*B*).

Generation of an ads1$^-$ *Knock-out*—An *ads1*$^-$ null mutant (Δ*ADS1*::*SAT*/Δ*ADS1*::*HYG*) was generated by two rounds of gene replacement since *Leishmania* is an asexual diploid (Ref. 31 and see Fig. 1, *C* and *D*, for predicted structures of replacements and Southern blot confirmation). These were recovered at typical frequencies, appeared morphologically to be normal, and grew well in culture with a doubling time of 8.1 *versus* 7 h for wild type (WT, Table I). As a control "add-back" line for subsequent studies, several *ads1*$^-$ mutants were transfected with the *ADS1*-expressing plasmid pXG-ADS1, yielding lines termed *ads1*$^-$/+*ADS1*. *ads1*$^-$ differentiated normally to the infective metacyclic stage (Table I) where it expressed stage-specific markers such as *SHERP* (Fig. 2*B*).

ADS activity was measured from enriched glycosomal preparations. WT showed high levels of activity, while *ads1*$^-$ showed only background levels, and *ads1*$^-$/+*ADS1* restored ADS activity to WT levels (Fig. 2*A*). Thus *ADS1* was responsible for cellular ADS activity.

The ads1$^-$ *Mutant Lacks Ether Phospholipids*—Total phospholipids from WT, *ads1*$^-$, and *ads1*$^-$/+*ADS1* cells were analyzed by ES-MS and ES-MS-CID-MS (42). The positive ion spectrum for WT was found to contain mainly PE and PC species (Fig. 3*A*, *upper panel*). The $[M + H]^+$ PE ions at *m/z* 728 and 730 were consistent with alkylacyl-PEs with a total of 36 carbons and two (*m/z* 730) or three (*m/z* 728) degrees of unsaturation (*i.e.* C36:2 and C36:3). Negative ion mass spectrometry (see below) of these lipid species showed that they were plasmenylethanolamines (*i.e.* alkenyl-acyl-PEs with monounsaturated C18:1 alkenyl chains). The ion at *m/z* 466 was most likely a lyso-PE with a single C18:1 fatty acid. The ions at *m/z* 828, 830, and 880 were PC species, most likely C40:9, C40:8, and C44:11 diacyl-PCs, respectively. These unusually large and unsaturated PC species were consistent with the abundance of C22:5, C22:6, C18:3, C18:2, and C18:1 fatty acids in the PC fraction (17). The PC-containing ions at *m/z* 518, 520, and 522 and *m/z* 568 and 570 represented lyso-PC species containing C18:3, C18:2, and C18:1 and C22:6 and C22:5 fatty acids, respectively. The abundance of phosphatidylserine species was below the limit of detection.

In the *ads1*$^-$ cells the positive ion spectrum was markedly different (Fig. 3*A*, *middle panel*). While the lyso-acyl- and diacyl-PC species remained, the alkylacyl-PEs were absent. These phospholipids were all restored in *ads1*$^-$/+*ADS1* (Fig. 3*A*, *lower panel*), establishing their dependence on *ADS1*.

Negative ion ES-MS and ES-MS-CID-MS were used to identify PI species (Fig. 3*B*, *upper panel*). The strong *m/z* 778 and 806 ions produced intense *m/z* 241 [inositol-1,2-cyclic phosphate]$^-$ and *m/z* 259 [inositol monophosphate]$^-$ daughter ions

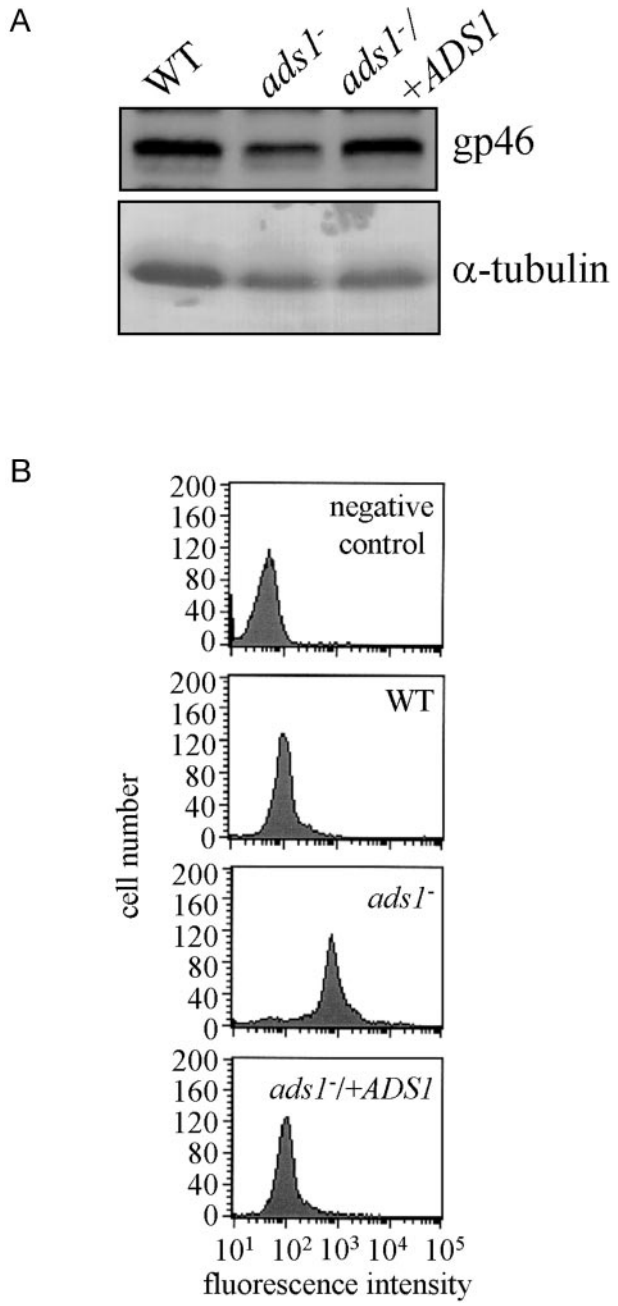

FIG. 5. **The *ads1*$^-$ mutant synthesizes normal levels of surface GPI-anchored protein gp46.** *A*, whole cell extracts (2×10^6 cells) from WT, *ads1*$^-$, and *ads1*$^-$/+*ADS1* lines were subjected to Western blot analysis with anti-gp46 or anti-α-tubulin antisera (*top* and *lower panel*, respectively). *B*, flow cytometry of fixed non-permeabilized parasites labeled with anti-gp46.

in ES-MS-CID-MS, a characteristic of inositol phosphorylceramides (50). Daughter ion spectra of *m/z* 849 and 933 confirmed their identities as alkylacyl-PI species as each ion fragmented to yield [inositol-1,2-cyclic phosphate]$^-$ (*m/z* 241), [*sn*-1-alkylglycerol-2,3-cyclic phosphate] (*m/z* 405 or 489), and C18:2 carboxylate ions (*m/z* 279) (data not shown). Of the remaining ions, *m/z* 728 and *m/z* 464 $[M - H]^-$ ions corresponded to the abundant *m/z* 730 and *m/z* 466 $[M + H]^+$ alkylacyl-PE and lyso-PE ions seen in the positive ion spectrum. The *m/z* 728 and 726 alkylacyl-PE $[M - H]^-$ parent ions were subjected to fragmentation, and the daughter ion spectra revealed the presence of *m/z* 464 1-*O*-(C18:1)alkenyl-2-lyso-PE fragment ions and *m/z* 281 (Fig. 3*C*) or *m/z* 279 fatty acid carboxylate ions, respectively. Thus, the major PEs are alkenylacyl-PEs. The

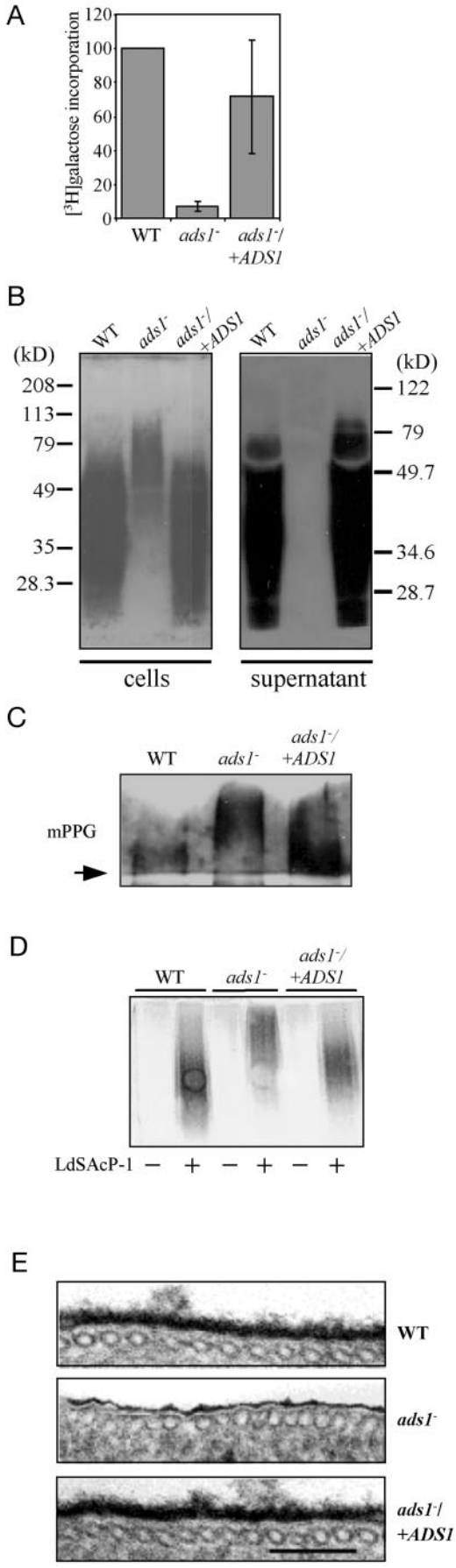

FIG. 6. **Phosphoglycan expression and glycocalyx structure in WT and *ads1*$^-$ *L. major*.** *A*, LPG was metabolically labeled with [^{3}H]Gal, purified, and quantified by liquid scintillation counting. Values are given relative to WT, and the S.D. is shown. *B*, whole cell extracts (1×10^6 cells) or cell supernatants (30 μl/lane) of a mid-log (5×10^6/ml) culture from WT, *ads1*$^-$, and *ads1*$^-$/+*ADS1* cells were separated by SDS-PAGE and subjected to immunoblotting with the anti-phosphoglycan antibody WIC79.3. Protein marker (kDa) is indicated. *C*, membrane proteophosphoglycans (*mPPG*) show decreased mobility in *ads1*$^-$ consistent with increased phosphoglycosylation. Proteophosphoglycans were resolved in the stacking gel by discontinuous 4%/10% SDS-PAGE and subjected to Western blotting with WIC79.3; the *arrow* marks the border between the stacking and separating gel. *D*, phosphoglycosylation of an *L. donovani* sAP PG "reporter" is elevated in the *ads1*$^-$ line. Culture supernatants from *L. major* WT, *ads1*$^-$, or *ads1*$^-$/+*ADS1* lines transfected with either pX63PAC (denoted by −) or pX63PAC-LdSAcP-1 (denoted by +) were separated by native PAGE and stained for acid phosphatase activity. *E*, transmission electron microscopy of the surface glycocalyx of WT, *ads1*$^-$, and *ads1*$^-$/+*ADS1* cells stained with ruthenium red for carbohydrate. The *bar* corresponds to 0.1 μm.

identity of the ion *m/z* 552 is unknown. The negative ion spectra of *ads1*$^-$ phospholipids (Fig. 3*B*, *middle panel*) lacked the alkylacyl-PI ions (at *m/z* 849 and 933) but contained four unidentified (non-inositolphospholipid) ion clusters at *m/z* 479, 504, 554, and 604. The spectrum for the *ads1*$^-$/+*ADS1* phospholipids (Fig. 3*B*, *lower panel*) showed restoration of the alkylacyl-PI ions and disappearance of the unidentified ions. As seen in the positive ion mode, these data established that lack of *ADS1* leads to complete loss of expression of ether phospholipids.

The ads1$^-$ *Mutant Lacks Conventional GIPLs*—The GIPL fraction of *ads1*$^-$/+*ADS1* cells was analyzed by positive ion ES-MS (Fig. 4*B*). The ions at *m/z* 1255/1283, 1417/1445, and 1579/1607 represented iM2, GIPL-1, and GIPL-2 species containing C18:0 alkyl and C12:0/C14:0 acyl chains, respectively (see Fig. 4*A* for structures) (51, 52). These assignments were confirmed by ES-MS-CID-MS (data not shown). In contrast, the *ads1*$^-$ spectrum showed that the GIPLs identified above were completely absent (Fig. 4*C*). Daughter ion analysis of the remaining peaks of *m/z* 1561 and 1582 showed that they were dimer ions ($[2M + H]^+$ and $[2M + Na]^+$, respectively) of inositol phosphorylceramide. Thus the *ads1*$^-$ lacked all conventional GIPLs.

Interestingly the *ads1*$^-$/+*ADS1* GIPL fraction also showed ions at *m/z* 1156 and 1318, whose ES-MS-CID-MS spectra identified them as lyso-iM2 and lyso-GIPL-1 species, respectively, with C24:0 alkyl chains. These latter species were LPG precursors that are barely detectable in WT cells (51), suggesting that overexpression of ADS1 in the *ads1*$^-$/+*ADS1* line may lead to their overproduction.

The ads1$^-$ *Mutant Synthesizes Normal Amounts of GPI-anchored Proteins*—We examined the synthesis of the abundant alkylacyl-GPI-anchored proteins gp46/PSA-2 and gp63 by immunoblots and flow cytometry. In contrast to the results obtained with GIPLs and ether phospholipids, the WT, *ads1*$^-$, and add-back strains synthesized similar levels of gp46 (Fig. 5*A*). gp46 was localized on the plasma membrane in *ads1*$^-$ where it showed enhanced fluorescence (Fig. 5*B*). This reflected the absence of LPG as seen previously (53) and as discussed below. Similar studies showed that gp63 steady state expression was not affected in the *ads1*$^-$ mutant (data not shown). Efforts to determine the structure of the gp63 anchor in *ads1*$^-$ were not successful (data not shown).

The ads1$^-$ *Mutant Lacks LPG*—Metabolic labeling of WT, *ads1*$^-$ and *ads1*$^-$/+*ADS1* parasites with [^{3}H]Gal followed by extraction and purification of the LPG fraction showed that *ads1*$^-$ contained about 7% of WT levels (Fig. 6*A*). LPG was visualized by Western blot analysis with the anti-PG monoclonal antibody WIC79.3 (54). LPG from WT and *ads1*$^-$/+*ADS1* lines migrated as a smear with an apparent molecular mass of 30–60 kDa both from cells and when shed into culture

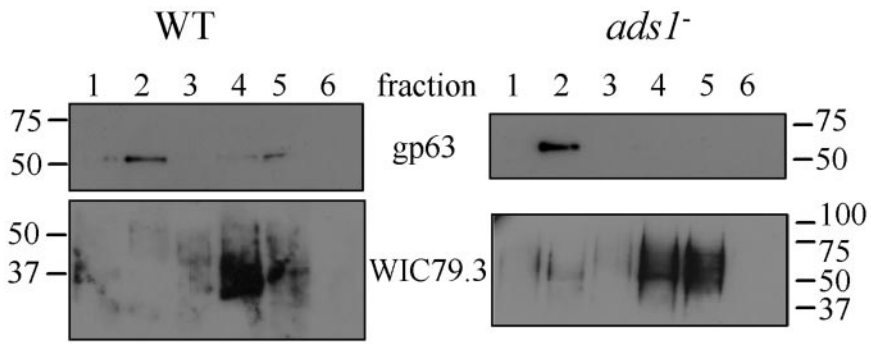

FIG. 7. **Ether lipids are not required for DRM/lipid raft formation in *ads1*⁻.** Cold Triton X-100-extracted DRMs from WT and *ads1*⁻ (*left* and *right panels*, respectively) parasites were fractionated on a density gradient (*fractions 1–6*, low to high density) and subjected to Western blotting with antisera against gp63 (*top panels*) or LPG (WIC79.3, *lower panels*). The size of the protein makers is indicated in kDa.

supernatants (Fig. 6*B*). *ads1*⁻ contained significantly less WIC79.3-reactive material (termed LPG-like), which had reduced electrophoretic mobility (50–100 kDa) and was not secreted into the medium (Fig. 6*B*). In contrast, Western blots showed similar levels of proteophosphoglycan in both WT and *ads1*⁻ (Fig. 6*C*), again with that of *ads1*⁻ showing reduced mobility. Analysis of the PG repeat structures by cone voltage fragmentation ES-MS (43) of LPG from WT and *ads1*⁻/+*ADS1* parasites and the LPG-like fraction of *ads1*⁻ showed that they were identical (data not shown). Attempts to determine the structure of a possible PI lipid component in purified preparations of the *ads1*⁻ LPG-like material by negative ion ES-MS analysis were unsuccessful.

LPG comprises a major portion of the parasite surface glycocalyx (55). Correspondingly transmission electron microscope analysis of plasma membranes stained with ruthenium red showed the typical LPG-rich glycocalyx for WT and *ads1*⁻/+*ADS1* parasites but relatively little staining in the *ads1*⁻ mutant (Fig. 6*E*). The absence of the surface glycocalyx in *ads1*⁻ conferred increased sensitivity to lysis by human complement (Table I) and labeling with antisera to GPI-anchored proteins (Fig. 5*B*).

Phosphoglycosylation Is More Extensive in ads1⁻ Mutants—The slower electrophoretic mobility of PG-containing molecules in *ads1*⁻ relative to WT suggested that they could be more extensively phosphoglycosylated (for a review, see Ref. 56). To test this, we used the *L. donovani* secretory acid phosphatase (sAP) gene *SAcP-1* as a "phosphoglycosylation reporter" following transfection into *L. major*. sAP lacks a GPI membrane anchor, and *L. major* normally expresses very low levels (57). *In situ* enzymatic activity assays showed that WT and the *ads1*⁻/+*ADS1 SAcP-1* transfectants expressed sAPs with identical electrophoretic mobility, while *ads1*⁻ transfectant sAPs migrated more slowly; as expected, vector transfectant controls lacked detectable sAP (Fig. 6*D*). This suggested that the degree of phosphoglycosylation was elevated in *ads1*⁻.

Increased phosphoglycosylation occurs during *Leishmania* development with higher numbers of PG repeats found in the LPG of metacyclic promastigotes (8, 58). However, metacyclogenesis and the stage-specific expression of the metacyclic marker *SHERP* were normal in *ads1*⁻ (Table I and Fig. 2*B*), suggesting that differentiation was not altered in this line.

ADS1 Is Not Required for Formation of Lipid Rafts (DRMs)—We asked whether the absence of ether lipids leads to alterations in the formation of "lipid rafts" as defined by buoyant DRM criteria. DRMs were prepared by standard procedures from log phase parasites and further separated on density gradients, and the distribution of LPG and gp63 into a buoyant fraction expected for lipid rafts was assessed. As previously observed, in WT *L. major* the GPI-anchored protein gp63 resides in a buoyant fraction (Fig. 7, *upper left panel*, *fraction 2*), whereas the majority of cellular material was found in dense fractions toward the bottom of the gradient (data not shown, Refs. 44 and 59). Similar results were obtained with *ads1*⁻ (Fig. 7, *upper right panel*), showing that DRM formation was not altered. In contrast, LPG did not reside in buoyant DRMs in either WT or *ads1*⁻ parasites (Fig. 7, *lower panels*). This conflicted with results reported previously in WT parasites (44) where LPG did show enrichment in the buoyant DRM fraction. This discrepancy was shown to reflect differences in the methods used in the previous study, which examined pulse-labeled cells treated with tunicamycin rather than steady state levels in the unperturbed cells as studied here.[2] Regardless the key finding was that DRMs did not differ between WT or *ads1*⁻ parasites.

ADS1 Is Important for Establishment of Infections in Mice and Macrophages—Following inoculation of stationary phase promastigotes into susceptible BALB/c mice, WT parasites formed lesions that appeared after ~15 days and progressed rapidly, while their appearance in *ads1*⁻ was delayed until 40 days and progressed somewhat more slowly thereafter (Fig. 8*A*). Lesion size correlated with the parasite burden (data not shown), and the *ads1*⁻/+*ADS1* line induced lesions in a manner similar to WT (Fig. 8*A*). *ads1*⁻ amastigotes were recovered from mice showing lesions around day 70, allowed to differentiate back to promastigotes, and reinoculated into animals, yielding identical results (data not shown). This showed that the delayed lesion appearance was not due to the presence of revertants or contaminants.

Macrophage infections were performed with stationary stage promastigotes parasites opsonized with C5-deficient mouse serum. While *ads1*⁻ parasites were taken up into macrophages somewhat better than WT (as seen previously in other LPG-deficient lines, Refs. 41 and 60), nearly 95% perished within 2 days of infection *versus* 30–50% for WT or the add-back strain (Fig. 8*B*, *top panel*). The extent of destruction was higher than seen previously with an LPG-deficient *lpg1*⁻ mutant (41, 61). Quantitation of the few surviving *ads1*⁻ parasites showed that they went on to replicate albeit at about 50% the rate seen in the WT or *ads1*⁻/+*ADS1* (Fig. 8*B*, *lower panel*).

ADS1 Is Not Required for Replication or Infection of Amastigotes—The promastigote infections of macrophages and mice suggested that while defective in establishment of infection those *ads1*⁻ parasites that escaped initial destruction during the "establishment phase" were able to survive and propagate as amastigotes. In this aspect *ads1*⁻ resembled the specifically LPG-deficient mutant *lpg1*⁻ (41, 61) where this was expected since the amastigote stage normally lacks LPG. Extrapolation to *ads1*⁻ would argue that ether lipids are not essential for replication as amastigotes.

To test this, *ads1*⁻ amastigotes were purified from mouse lesions similar to those shown in Fig. 8*A* and then used to initiate macrophage infections directly. In contrast to the re-

[2] P. Denny and D. F. Smith, unpublished.

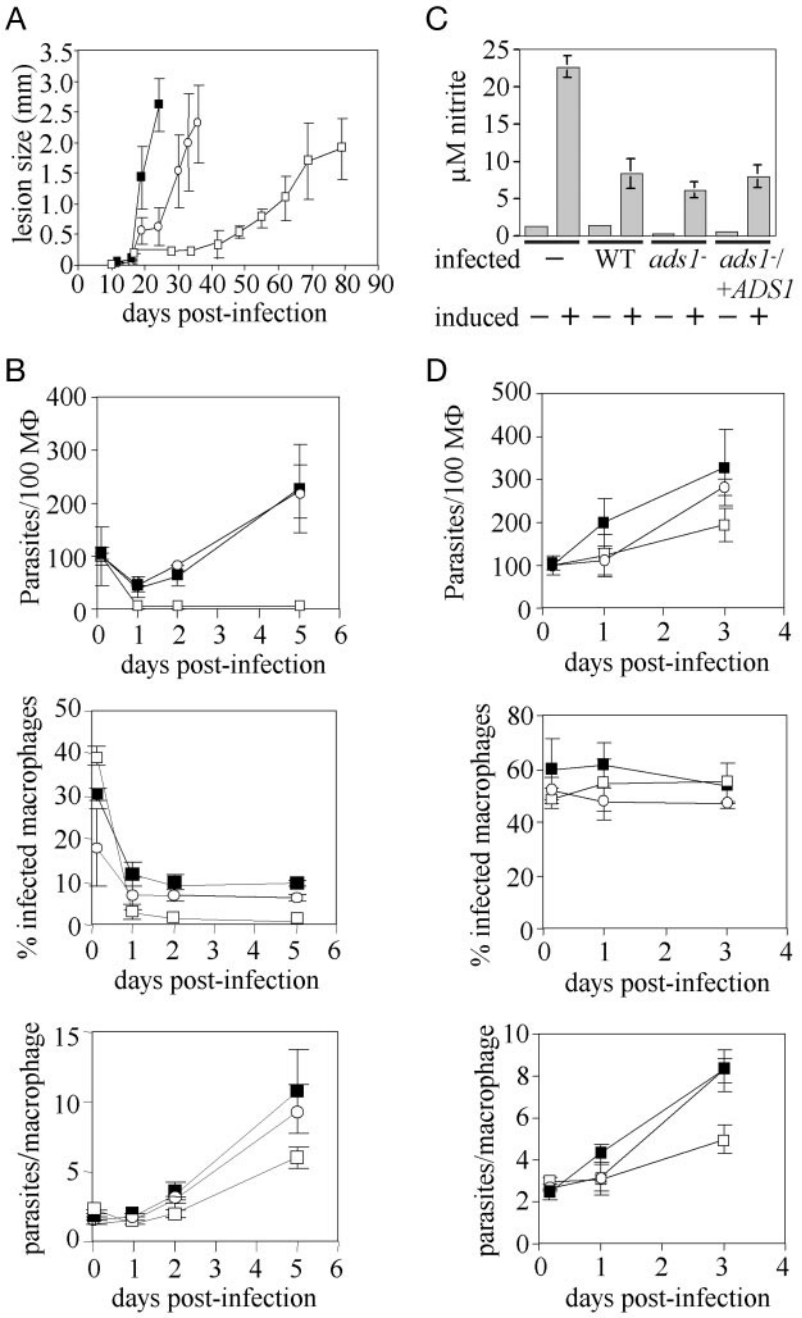

FIG. 8. **Ether lipids are important for the establishment of macrophage infections by *ads1*$^-$ but not for amastigote virulence or for inhibition of NO production by macrophages.** *A*, lesion formation following footpad inoculation of 1×10^6 stationary phase promastigotes (WT, ■; *ads1*$^-$, □; *ads1*$^-$/+*ADS1*, ○). *B*, *in vitro* macrophage infection with C3-opsonized stationary phase promastigotes. The survival of parasites/100 macrophages (*M*Φ) and the percentage of infected macrophages as a function of time is indicated in the *upper* and *middle panels*, respectively; the growth of the surviving intracellular parasites (parasites/infected macrophage) is shown in the *lower panel*. These results were derived from two independent triplicate experiments. *Symbols* are as in *A*. *C*, NO synthesis. Macrophages were infected with the indicated strains in triplicate *in vitro*; after 6 h, interferon-γ and lipopolysaccharide were added to the cultures marked with a +, and the incubation was continued another 48 h. Nitrite levels and S.D. are shown. *D*, *in vitro* macrophage infection with amastigote parasites freshly isolated from a mouse footpad lesion; the data are presented as described in *B*.

sults obtained with stationary phase promastigote infections, *ads1*$^-$ amastigotes entered and survived well in macrophages and went on to replicate well albeit again at about one-third the rate seen in WT or *ads1*$^-$/+*ADS1* (Fig. 8*D* and Table I). Similar findings were obtained in mouse infections by amastigotes (data not shown).

ads1$^-$ *Retained the Ability to Inhibit Macrophage NO Production*—Purified metacyclic parasites were used to infect two sets of peritoneal macrophages; after 6 h, interferon-γ and lipopolysaccharide were added to one set of infected macrophages, and NO production was determined. As expected, infections with WT *L. major* did not induce NO synthesis, and these parasites inhibited macrophage NO production by 70% following treatment with activators (Fig. 8*C*); similar results arose with the control *ads1*$^-$/+*ADS1*. Surprisingly *ads1*$^-$ showed the same profile even though the overwhelming majority of these parasites were destroyed by macrophages (Fig. 8, *B* and *C*).

DISCUSSION

In this work we used multiple approaches to establish that the *Leishmania* alkyl-DHAP synthase encoded by *ADS1* is required for all cellular ether phospholipid synthesis and to explore its role in parasite biology. Despite the fact that more than 10% of *Leishmania* cellular lipids are comprised by ether phospholipids, the *ads1*$^-$ null mutant was viable. Enzymatic studies showed that ADS activity was absent in *ads1*$^-$, and biochemical studies showed that all known ether phospholipid species were lacking. These included alkenylacyl-PEs as well as GPI-anchored molecules such as LPG and GIPLs. In this respect *ads1*$^-$ differs from previously identified mammalian mutants defective in ether lipid biosynthesis that are typically "leaky" and express residual levels of plasmalogens (21). While GPI-anchored proteins were retained at the parasite surface at normal levels, it seems likely that they now contain an alternative lipid anchor, probably diacylglycerol (as seen in trypano-

some variant surface glycoproteins), although efforts to confirm this were inconclusive. Since no other specific alterations in lipid composition were seen in *ads1*$^-$, we presume that that a modest up-regulation of remaining membrane lipid species compensated for the general lack of ether phospholipids.

Remarkably the complete loss of ether phospholipids, LPG, and GIPLs was accompanied by minimal changes in many aspects of parasite biology: for example, only a modest reduction in growth rate was observed *in vitro* as promastigotes or as amastigotes within macrophages *in vivo*. A secondary phenotype was increased phosphoglycosylation of endogenous or reporter proteins in the *ads1*$^-$ mutant. Its basis was not sought; it may arise from small differences in membrane vesicular trafficking dependent upon ether lipids as seen in mammalian cells (62, 63).

Previous studies have shown that ether lipids can associate and potentially contribute to the stability of membrane microdomains commonly termed lipid rafts, which are also rich in sterols and sphingolipids (64–68). However, lipid rafts (as defined by DRM criteria) were maintained in *ads1*$^-$ in the absence of the 10% of cellular lipids comprised by *Leishmania* ether phospholipids, possibly reflecting the ameliorating abundance of sphingolipids and especially ergosterol in the parasite membrane (17, 19). It should be emphasized that retention of DRMs does not necessarily imply that the lipid rafts remaining in *ads1*$^-$ are identical to those of WT; to address this, additional markers for parasite rafts will have to be identified and examined in the future.

The synthesis of the major classes of GPI-anchored molecules has been proposed to diverge from a common Man-GlcN-PI precursor (3, 69) with LPG and type 2 GIPLs requiring the formation of Man(α1–3)Man-GlcN-PI and protein GPI anchors requiring the formation of Man(α1–6)Man-GlcN-PI. The loss of LPG/GIPL but not protein GPI anchor synthesis in the *ads1*$^-$ line suggests that the GDP-Man:Man-GlcN-PI (α1–3) mannosyltransferase may be dependent on Man-GlcN-PI acceptors that contain *sn*-1-alkyl-2-acyl-PI, whereas the dolichol-phosphoryl-Man:Man-GlcN-PI (α1–6) mannosyltransferase may also function with diacyl-PI-containing acceptors. Consistent with this model, [^{3}H]GlcN labeling studies have shown that GlcN-diacyl-PIs are synthesized by *L. major* promastigotes (70), providing potential non-ether lipid substrates for protein GPI anchor synthesis, and cell-free GPI biosynthesis studies have suggested that the GDP-Man:Man-GlcN-PI (α1–3) mannosyltransferase may not act on Man-GlcN-diacyl-PI (3). There are precedents for lipid specificity/selectivity for certain mammalian GPI biosynthetic enzymes, although GPI anchor synthesis in *T. brucei* shows a relaxed specificity for the composition of the lipid anchor (71, 72). Future studies may explore the lipid specificity of LPG/GIPL and protein GPI anchor synthesis in *L. major* in more detail.

The abundance of GIPLs in the intracellular amastigote stage (3, 73) and the ability of purified GPI anchors and GIPLs to modulate key signaling pathways implicated in parasite survival in macrophages (5, 7) led to proposals that these molecules play major roles in parasite virulence. However, genetic studies of GIPL function in *Leishmania mexicana* have yielded contradictory results possibly because they were based upon mutants with broad and complex effects beyond GIPL synthesis (9, 11, 74, 75). Moreover *L. mexicana* and *L. major* differ greatly in their dependence upon LPG and phosphoglycans for virulence probably due to interactions with the host immune response (76). The *L. major ads1*$^-$ mutant studied here affected a defined set of parasite ether phospholipids in a species in which for both LPG and PGs the general roles in virulence and the specific mechanisms by which these act have been defined genetically (41, 61).

Remarkably the phenotype seen for *L. major ads1*$^-$ was nearly indistinguishable from the LPG-deficient mutant *lpg1*$^-$: both showed increased sensitivity to lysis by complement due to disruption of the glycocalyx, normal metacyclogenesis, increased destruction following macrophage infection, and delayed lesion appearance (Table I and Figs. 2*B* and *8* and Refs. 41 and 61). That the *ads1*$^-$ phenotype included the *lpg1*$^-$ phenotype was not surprising given that it lacks LPG, but that the absence of both GIPLs and ether phospholipids conferred little additional effect was unexpected especially in the amastigote stage. In contrast, the globally PG-deficient *L. major* mutant *lpg2*$^-$ was unable to establish macrophage infections at all and did not induce pathology in mouse infections (60). We conclude therefore that neither GIPL nor ether phospholipid synthesis is uniquely required for amastigote growth and survival in macrophages *in vitro* or in mouse infections *in vivo*.

Similarly we found that despite its attenuated ability to establish infections in macrophages, the *ads1*$^-$ mutant did not induce NO following entry and inhibited the ability of macrophages to make NO following the strong induction signal of interferon-γ plus lipopolysaccharide (Fig. 8*C*). This was remarkable given reports that the alkylglycerol anchor of LPG or the alkylacyl anchor of GIPLs can inhibit macrophage activation pathways leading to the activation of protein kinase C and/or the formation of NO or interleukin-12 (4–7). There are a number of potential explanations. One is that the highly purified GPIs studied previously contained traces of an active, non-GPI species. Similar problems were encountered in assessing the antigenicity of purified LPG preparations (77). A second possibility is that differences in the amount, form, or delivery route of GPI-anchored molecules tested *in vitro* does not closely mimic what occurs in natural infection *in vivo*. A third possibility invokes redundancy of GIPL functions with those of other parasite molecules as it seems likely during evolution that selection for multiple mechanisms ensuring repression of macrophage activation would be advantageous. Reasonable candidates for this role might be other parasite glycolipids such as sphingolipids or protein-GPI anchor moieties remaining in *ads1*$^-$, and the possibility of molecules other than glycolipids cannot be excluded.

Acknowledgments—We thank D. G. Russell, B. Ullman, and D. McMahon-Pratt for the generous gift of gp63 (235), α-tubulin, hypoxanthine guanine phosphoribosyltransferase, and gp46 antibodies; D. S. Ha for making pXGSAT; D. Dwyer for plasmid pLdSAcP3.9; A. K. Hajra for providing labeled hexadecanol; F. Opperdoes, N. Heise, and G. Späth for discussions; and A. Capul, D. Dobson, and K. Zhang for comments on this manuscript.

REFERENCES

1. Ferguson, M. A. (1997) *Philos. Trans. R. Soc. Lond. B Biol. Sci.* **352,** 1295–1302
2. Ilgoutz, S. C., and McConville, M. J. (2001) *Int. J. Parasitol.* **31,** 899–908
3. McConville, M. J., Mullin, K. A., Ilgoutz, S. C., and Teasdale, R. D. (2002) *Microbiol. Mol. Biol. Rev.* **66,** 122–154
4. Chawla, M., and Vishwakarma, R. A. (2003) *J. Lipid Res.* **44,** 594–600
5. Proudfoot, L., O'Donnell, C. A., and Liew, F. Y. (1995) *Eur. J. Immunol.* **25,** 745–750
6. Tachado, S. D., Mazhari-Tabrizi, R., and Schofield, L. (1999) *Parasite Immunol. (Oxf.)* **21,** 609–617
7. McNeely, T. B., Rosen, G., Londner, M. V., and Turco, S. J. (1989) *Biochem. J.* **259,** 601–604
8. Moody, S. F., Handman, E., McConville, M. J., and Bacic, A. (1993) *J. Biol. Chem.* **268,** 18457–18466
9. Ilgoutz, S. C., Zawadzki, J. L., Ralton, J. E., and McConville, M. J. (1999) *EMBO J.* **18,** 2746–2755
10. McConville, M. J., and Bacic, A. (1989) *J. Biol. Chem.* **264,** 757–766
11. Mensa-Wilmot, K., Garg, N., McGwire, B. S., Lu, H. G., Zhong, L., Armah, D. A., LeBowitz, J. H., and Chang, K. P. (1999) *Mol. Biochem. Parasitol.* **99,** 103–116
12. McConville, M. J., Thomas-Oates, J. E., Ferguson, M. A., and Homans, S. W. (1990) *J. Biol. Chem.* **265,** 19611–19623
13. Orlandi, P. A., Jr., and Turco, S. J. (1987) *J. Biol. Chem.* **262,** 10384–10391
14. Turco, S. J. (1999) *Parasite Immunol. (Oxf.)* **21,** 597–600
15. Proudfoot, L., Nikolaev, A. V., Feng, G. J., Wei, W. Q., Ferguson, M. A., Brimacombe, J. S., and Liew, F. Y. (1996) *Proc. Natl. Acad. Sci. U. S. A.* **93,**

10984–10989
16. Tachado, S. D., Gerold, P., McConville, M. J., Baldwin, T., Quilici, D., Schwarz, R. T., and Schofield, L. (1996) *J. Immunol.* **156,** 1897–1907
17. Beach, D. H., Holz, G. G., Jr., and Anekwe, G. E. (1979) *J. Parasitol.* **65,** 201–216
18. Singh, B. N., Costello, C. E., Beach, D. H., and Holz, G. G., Jr. (1988) *Biochem. Biophys. Res. Commun.* **157,** 1239–1246
19. Wassef, M. K., Fioretti, T. B., and Dwyer, D. M. (1985) *Lipids* **20,** 108–115
20. Croft, S. L., Seifert, K., and Duchene, M. (2003) *Mol. Biochem. Parasitol.* **126,** 165–172
21. Nagan, N., and Zoeller, R. A. (2001) *Prog. Lipid Res.* **40,** 199–229
22. Heise, N., and Opperdoes, F. R. (1997) *Mol. Biochem. Parasitol.* **89,** 61–72
23. Lux, H., Heise, N., Klenner, T., Hart, D., and Opperdoes, F. R. (2000) *Mol. Biochem. Parasitol.* **111,** 1–14
24. Opperdoes, F. R., and Michels, P. A. (1993) *Biochimie* (*Paris*) **75,** 231–234
25. van den Bosch, H., and de Vet, E. C. (1997) *Biochim. Biophys. Acta* **1348,** 35–44
26. Zomer, A. W., Michels, P. A., and Opperdoes, F. R. (1999) *Mol. Biochem. Parasitol.* **104,** 55–66
27. Kapler, G. M., Coburn, C. M., and Beverley, S. M. (1990) *Mol. Cell. Biol.* **10,** 1084–1094
28. Späth, G. F., and Beverley, S. M. (2001) *Exp. Parasitol.* **99,** 97–103
29. Sambrook, J., Fritsch, E. F., and Maniatis, T. (1989) *Molecular Cloning: A Laboratory Manual*, Cold Spring Harbor Laboratory, Cold Spring Harbor, NY
30. Ryan, K. A., Dasgupta, S., and Beverley, S. M. (1993) *Gene* (*Amst.*) **131,** 145–150
31. Cruz, A., Coburn, C. M., and Beverley, S. M. (1991) *Proc. Natl. Acad. Sci. U. S. A.* **88,** 7170–7174
32. Joshi, P. B., Webb, J. R., Davies, J. E., and McMaster, W. R. (1995) *Gene* (*Amst.*) **156,** 145–149
33. Ha, D. S., Schwarz, J. K., Turco, S. J., and Beverley, S. M. (1996) *Mol. Biochem. Parasitol.* **77,** 57–64
34. Shakarian, A. M., Ellis, S. L., Mallinson, D. J., Olafson, R. W., and Dwyer, D. M. (1997) *Gene* (*Amst.*) **196,** 127–137
35. Schrakamp, G., Roosenboom, C. F., Schutgens, R. B., Wanders, R. J., Heymans, H. S., Tager, J. M., and van den Bosch, H. (1985) *J. Lipid Res.* **26,** 867–873
36. Ryu, E. K., and MacCoss, M. (1979) *J. Lipid Res.* **20,** 561–563
37. Laemmli, U. K. (1970) *Nature* **227,** 680–685
38. Katakura, K., and Kobayashi, A. (1988) *Infect. Immun.* **56,** 2856–2860
39. Shih, S., Hwang, H. Y., Carter, D., Stenberg, P., and Ullman, B. (1998) *J. Biol. Chem.* **273,** 1534–1541
40. Tolson, D. L., Turco, S. J., Beecroft, R. P., and Pearson, T. W. (1989) *Mol. Biochem. Parasitol.* **35,** 109–118
41. Späth, G. F., Epstein, L., Leader, B., Singer, S. M., Avila, H. A., Turco, S. J., and Beverley, S. M. (2000) *Proc. Natl. Acad. Sci. U. S. A.* **97,** 9258–9263
42. Schneiter, R., Brugger, B., Sandhoff, R., Zellnig, G., Leber, A., Lampl, M., Athenstaedt, K., Hrastnik, C., Eder, S., Daum, G., Paltauf, F., Wieland, F. T., and Kohlwein, S. D. (1999) *J. Cell Biol.* **146,** 741–754
43. Wilson, I. B., O'Donnell, N., Allen, S., Mehlert, A., and Ferguson, M. A. (1999) *Mol. Biochem. Parasitol.* **100,** 207–215
44. Denny, P. W., Field, M. C., and Smith, D. F. (2001) *FEBS Lett.* **491,** 148–153
45. Titus, R. G., Marchand, M., Boon, T., and Louis, J. A. (1985) *Parasite Immunol.* (*Oxf.*) **7,** 545–555
46. Racoosin, E. L., and Beverley, S. M. (1997) *Exp. Parasitol.* **85,** 283–295
47. Green, L. C., Wagner, D. A., Glogowski, J., Skipper, P. L., Wishnok, J. S., and Tannenbaum, S. R. (1982) *Anal. Biochem.* **126,** 131–138
48. Sommer, J. M., and Wang, C. C. (1994) *Annu. Rev. Microbiol.* **48,** 105–138
49. Clayton, C. E. (2002) *EMBO J.* **21,** 1881–1888
50. Serrano, A. A., Schenkman, S., Yoshida, N., Mehlert, A., Richardson, J. M., and Ferguson, M. A. (1995) *J. Biol. Chem.* **270,** 27244–27253
51. McConville, M. J., Homans, S. W., Thomas-Oates, J. E., Dell, A., and Bacic, A. (1990) *J. Biol. Chem.* **265,** 7385–7394
52. Schneider, P., Schnur, L. F., Jaffe, C. L., Ferguson, M. A., and McConville, M. J. (1994) *Biochem. J.* **304,** 603–609
53. Karp, C. L., Turco, S. J., and Sacks, D. L. (1991) *J. Immunol.* **147,** 680–684
54. de Ibarra, A. A., Howard, J. G., and Snary, D. (1982) *Parasitology* **85,** 523–531
55. Pimenta, P. F., Saraiva, E. M., and Sacks, D. L. (1991) *Exp. Parasitol.* **72,** 191–204
56. Mengeling, B. J., Beverley, S. M., and Turco, S. J. (1997) *Glycobiology* **7,** 873–880
57. Shakarian, A. M., and Dwyer, D. M. (2000) *Exp. Parasitol.* **95,** 79–84
58. McConville, M. J., Turco, S. J., Ferguson, M. A., and Sacks, D. L. (1992) *EMBO J.* **11,** 3593–3600
59. Ralton, J. E., Mullin, K. A., and McConville, M. J. (2002) *Biochem. J.* **363,** 365–375
60. Späth, G. F., Lye, L. F., Segawa, H., Sacks, D. L., Turco, S. J., and Beverley, S. M. (2003) *Science* **301,** 1241–1243
61. Späth, G. F., Garraway, L. A., Turco, S. J., and Beverley, S. M. (2003) *Proc. Natl. Acad. Sci. U. S. A.* **100,** 9536–9541
62. Glaser, P. E., and Gross, R. W. (1995) *Biochemistry* **34,** 12193–12203
63. Thai, T. P., Rodemer, C., Jauch, A., Hunziker, A., Moser, A., Gorgas, K., and Just, W. W. (2001) *Hum. Mol. Genet.* **10,** 127–136
64. Ohvo-Rekila, H., Ramstedt, B., Leppimaki, P., and Slotte, J. P. (2002) *Prog. Lipid Res.* **41,** 66–97
65. Mattjus, P., and Slotte, J. P. (1996) *Chem. Phys. Lipids* **81,** 69–80
66. Simons, K., and Ikonen, E. (1997) *Nature* **387,** 569–572
67. Brown, D. A., and London, E. (2000) *J. Biol. Chem.* **275,** 17221–17224
68. Pike, L. J., Han, X., Chung, K. N., and Gross, R. W. (2002) *Biochemistry* **41,** 2075–2088
69. Ralton, J. E., and McConville, M. J. (1998) *J. Biol. Chem.* **273,** 4245–4257
70. Proudfoot, L., Schneider, P., Ferguson, M. A., and McConville, M. J. (1995) *Biochem. J.* **308,** 45–55
71. Watanabe, R., Inoue, N., Westfall, B., Taron, C. H., Orlean, P., Takeda, J., and Kinoshita, T. (1998) *EMBO J.* **17,** 877–885
72. Smith, T. K., Crossman, A., Paterson, M. J., Borissow, C. N., Brimacombe, J. S., and Ferguson, M. A. (2002) *J. Biol. Chem.* **277,** 37147–37153
73. Schneider, P., Rosat, J. P., Ransijn, A., Ferguson, M. A., and McConville, M. J. (1993) *Biochem. J.* **295,** 555–564
74. Garami, A., and Ilg, T. (2001) *EMBO J.* **20,** 3657–3666
75. Garami, A., Mehlert, A., and Ilg, T. (2001) *Mol. Cell. Biol.* **21,** 8168–8183
76. Turco, S. J., Späth, G. F., and Beverley, S. M. (2001) *Trends Parasitol.* **17,** 223–226
77. Jardim, A., Tolson, D. L., Turco, S. J., Pearson, T. W., and Olafson, R. W. (1991) *J. Immunol.* **147,** 3538–3544